LBL-13739
Preprint

Lawrence Berkeley Laboratory
UNIVERSITY OF CALIFORNIA

Materials & Molecular Research Division

RECEIVED
LAWRENCE
BERKELEY LABORATORY

JAN 20 1982

LIBRARY AND
DOCUMENTS SECTION

To be submitted for publication

MEASUREMENT OF THE DENSITY DEPENDENCE OF THE ELECTRON-HOLE LIQUID ENHANCEMENT FACTOR IN Ge

J.C. Culbertson and J.E. Furneaux

December 1981

TWO-WEEK LOAN COPY

This is a Library Circulating Copy which may be borrowed for two weeks. For a personal retention copy, call Tech. Info. Division, Ext. 6782

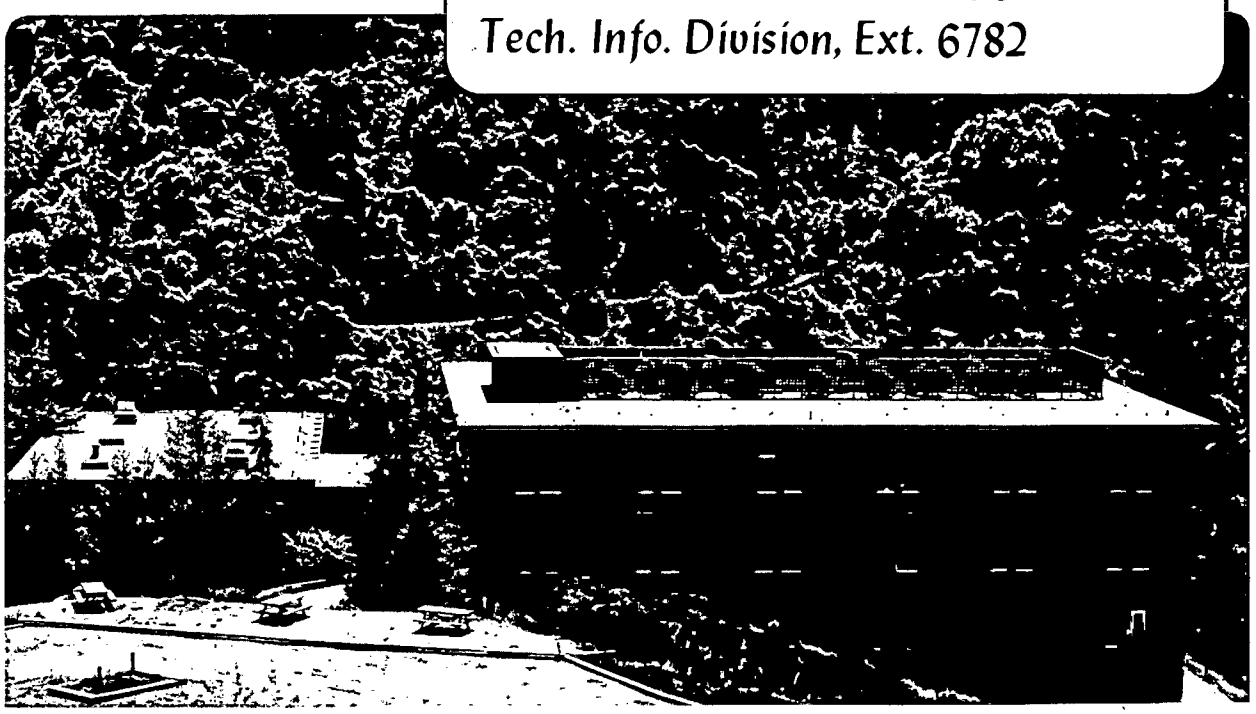

LBL-13739 c.2

Prepared for the U.S. Department of Energy under Contract W-7405-ENG-48

DISCLAIMER

This document was prepared as an account of work sponsored by the United States Government. While this document is believed to contain correct information, neither the United States Government nor any agency thereof, nor the Regents of the University of California, nor any of their employees, makes any warranty, express or implied, or assumes any legal responsibility for the accuracy, completeness, or usefulness of any information, apparatus, product, or process disclosed, or represents that its use would not infringe privately owned rights. Reference herein to any specific commercial product, process, or service by its trade name, trademark, manufacturer, or otherwise, does not necessarily constitute or imply its endorsement, recommendation, or favoring by the United States Government or any agency thereof, or the Regents of the University of California. The views and opinions of authors expressed herein do not necessarily state or reflect those of the United States Government or any agency thereof or the Regents of the University of California.

LBL-13739

MEASUREMENT OF THE DENSITY DEPENDENCE OF THE ELECTRON-HOLE LIQUID ENHANCEMENT FACTOR IN Ge*

J. C. CULBERTSON and J. E. FURNEAUX†

Materials and Molecular Research Division, Lawrence Berkeley Laboratory, and Department of Physics, University of California, Berkeley, CA 94720

December 1981

*This work was supported by the Director, Office of Energy Research, Office of Basic Energy Sciences, Materials Sciences Division of the U.S. Department of Energy under Contract Number W-7405-ENG-48.

†Present address: Code 6873, Naval Research Laboratory, Washington, D.C. 20375.

MEASUREMENT OF THE DENSITY DEPENDENCE OF THE ELECTRON-HOLE LIQUID ENHANCEMENT FACTOR IN Ge*

J. C. Culbertson and J. E. Furneaux†

Materials and Molecular Research Division, Lawrence Berkeley Laboratory, and Department of Physics, University of California, Berkeley, CA 94720

ABSTRACT

We report the first absolute measurement of the density dependence of the electron-hole liquid (EHL) enhancement factor in Ge. The enhancement factor, the ratio of the electron density at the site of a hole to the mean EHL density, provides a valuable and sensitive test for the predictions of various many body approximations. Our results, derived from measurements on a free exciton, EHL system confined to a strain induced potential well, are compared with predictions.

---

*This work was supported by the Director, Office of Energy Research, Office of Basic Energy Sciences, Materials Sciences Division of the U.S. Department of Energy under Contract Number W-7405-ENG-48.

†Present address: Code 6873, Naval Research Laboratory, Washington, D.C. 20375.

I. INTRODUCTION

The purpose of this paper is to report the first absolute measurement of the density dependence of the electron-hole liquid (EHL) enhancement factor $g_{eh}(o)$ in Ge. In this paper the importance of such a measurement, the measurement scheme and its validity are discussed, followed by experimental details, data, and results compared to predictions.[1]

To enhance the utility of many body theory calculations, it is essential to compare the results of various approximation schemes with experiment. The EHL provides a uniquely useful physical system to test many body theory approximations. The EHL is a two component electron-hole (e-h) Fermi liquid which exists in optically excited Ge at liquid helium temperatures. The EHL droplets studied generally contain many millions of e-h pairs. Various EHL parameters, such as binding energy and density, can easily be varied in the laboratory. The EHL density, for example, can be varied by applying stress, applying a magnetic field, or changing the temperature of the crystal containing the EHL. By applying stress, density variations of over a factor of 10 are achievable. The characteristics of the EHL system are known exactly,[1] and the many body calculation results are not small corrections. Other Fermi liquids such as neutron stars, nuclei, and electrons in metals suffer from various disadvantages such as the inability of the experimenter to alter parameters, small numbers of constituent particles, many body effects being small corrections, or the system's characteristics aren't known exactly for the purpose of theoretical calculations.

In this experiment we measure the e-h correlation function $g_{eh}(\vec{r})$ evaluated at zero electron-hole separation as a function of EHL density.

This correlation function $g_{eh}(o)$, normalized to one for a completely uncorrelated e-h plasma, is simply the ratio of the electron density on the hole to the mean density. If $g_{eh}(o) = 2$, then the probability per unit volume of finding an electron on a hole is enhanced by a factor of two over the probability for an uncorrelated plasma of the same density. This has led the labeling of $g_{eh}(o)$ as the enhancement factor.

Recall that in elementary perturbation theory a calculation of an energy eigenvalue is accurate to second order when evaluated using first order wave functions. One can determine good energy eigenvalues using relatively poor wave functions. Thus a wave function measurement provides a more sensitive check of an approximation scheme than does an energy eigenvalue. In the same spirit the enhancement factor $g_{eh}(o)$ which is a wave function measurement provides a valuable and sensitive test for the predictions of many body theory.

One other experiment[2] which measures $g_{eh}(o)$ vs EHL density n_L has been performed. Their results provide $g_{eh}(o)$ times some undetermined constant as a function of EHL density. In addition, their results depend on a model of how the EHL lifetime τ_L depends on the EHL density n_L that is at odds with the results of Kelso and Furneaux.[3]

Our experiment provides for the first time an absolute measurement of $g_{eh}(o)$ vs n_L and the extraction of $g_{eh}(o)$ from the data requires no model of τ_L (n_L).

II. MEASUREMENT SCHEME

The radiative decay rate $\frac{1}{\tau_{RL}}$ of the EHL is related to the probability of an electron being at the site of a hole and thus to the enhancement factor $g_{eh}(o)$. From the Guillaume-Voos[4] treatment of the radiative decay

rates of free excitons $\frac{1}{\tau_{RX}}$ and electron-hole liquid $\frac{1}{\tau_{RL}}$, we have

$$\frac{\tau_{RX}}{\tau_{RL}} = \frac{g_{eh}(o)n_L}{|\psi_X(o)|^2} \tag{1}$$

where $|\psi_X(o)|^2 = \frac{1}{\pi a_X^3}$ refers to the free exciton (FE) ground state wave function and a_X is the FE Bohr radius. Solving for $g_{eh}(o)$, we have

$$g_{eh}(o) = \frac{\tau_{RX}}{\tau_{RL}} \frac{|\psi_X(o)|^2}{n_L} \tag{2}$$

Defining radiative efficiencies for the EHL and FE

$$\varepsilon_{RL} = \frac{\left(\frac{1}{\tau_{RL}}\right)}{\left(\frac{1}{\tau_L}\right)} \quad \text{and} \quad \varepsilon_{RX} = \frac{\left(\frac{1}{\tau_{RX}}\right)}{\left(\frac{1}{\tau_X}\right)} \tag{3}$$

and incorporating these definitions into Eqn. (2) we have

$$g_{eh}(o) = \left(\frac{\varepsilon_{RL}}{\varepsilon_{RX}}\right) \frac{\tau_X}{\tau_L} \frac{|\psi_X(o)|^2}{n_L} \tag{4}$$

Of the terms on the right-hand side of Eqn. (4), $|\psi_X(o)|^2 = \frac{1}{\pi a_X^3}$ is a theoretical number and the rest are accessible to experiment. The lifetimes τ_X and τ_L are measured from luminescence decay, the EHL density n_L from EHL luminescence lineshape fitting, and the radiative efficiency ratio from a ratio of slopes in a steady state luminescence vs. excitation power experiment as explained below.

Consider a steady state experiment measuring the luminescence intensity of both free excitons I_X and electron-hole liquid I_L as a function of the e-h pair generation rate. We consider separately two cases: (a) below EHL threshold; (b) above EHL threshold.

(a) Below EHL threshold the EHL isn't present and the steady state number of free excitons N_X is determined by

$$G = \frac{N_X}{\tau_X} . \tag{5}$$

The measured luminescence I_X is related to N_X by

$$I_X = \frac{N_X}{\tau_{RX}} \varepsilon_{CX} \tag{6}$$

where the FE collection efficiency ε_{CX} relates the total FE luminescence emitted to that collected and detected. A collection efficiency for EHL is similarly defined. Combining Eqns. (5) and (6) we find that the luminescence to generation rate slope below EHL threshold is

$$\frac{dI}{dG} = \frac{dI_X}{dG} = \varepsilon_{RX} \varepsilon_{CX} \tag{7}$$

(b) Above EHL threshold both FE and EHL exist and the number of free excitons N_X and e-h pairs in the electron-hole liquid N_L are related to the generation rate G by

$$G = \frac{N_X}{\tau_X} + \frac{N_L}{\tau_L} \tag{8}$$

The measured EHL luminescence I_L is related to N_L by

$$I_L = \left(\frac{N_L}{\tau_{RL}}\right)\varepsilon_{CL} \tag{9}$$

where ε_{CX} is the EHL luminescence collection efficiency. The number of excitons N_X is related to I_X as in Eqn. (6). Just above EHL threshold $I_X \approx$ constant and the luminescence to generation rate slope is

$$\frac{dI}{dG} = \frac{dI_L}{dG} = \varepsilon_{RL} \varepsilon_{CL} \tag{10}$$

Any slope in I_X vs. G above EHL threshold can be measured and subtracted out. Taking the ratio of Eqn. (10) to Eqn. (7) we find

$$\frac{\left(\frac{dI}{dG}\right)_{\substack{\text{above EHL}\\ \text{threshold}}}}{\left(\frac{dI}{dG}\right)_{\substack{\text{below EHL}\\ \text{threshold}}}} = \left(\frac{\varepsilon_{RL}}{\varepsilon_{RX}}\right)\left(\frac{\varepsilon_{CL}}{\varepsilon_{CX}}\right) \tag{11}$$

Thus if we measure the slopes above to below EHL threshold of a total luminescence vs. generation rate scan and correct for the relative collection efficiencies of the FE and EHL luminescence we obtain the desired radiative efficiency ratio.

III. MEASUREMENT SCHEME VALIDITY

An assumption inherent in the use of steady state and decay measurements for the terms in Eqn. (4) is the existence of a thermal and diffusive quasi-equilibrium within the FE, EHL system. To compare steady state and decay measurements, the measurements must be made on the same physical system.

The physical system used in this experiment is a FE gas and at most one EHL droplet confined to a strain induced potential well[5,6] at a temperature 2.16K.

Three criteria must be satisfied for the FE, EHL system to be in quasi-equilibrium.

a) The e-h pairs in the EHL droplet must be in thermal and diffusive equilibrium.

b) The FE gas must be in thermal and diffusive equilibrium with itself.

c) The net current of FE pairs out of (for decays) or into (for steady state) the EHL droplet must be small compared to the equilibrium back and forth flux across the EHL droplet surface.

If any one of these conditions isn't met, then thermodynamics isn't sufficient and transport needs to be considered.

The carrier-phonon scattering time $\tau_P \sim 10^{-10}$ sec. so FE and EHL are well characterized by the same temperature for the very low excitation powers and long time scales of this experiment. The EHL droplet is a highly correlated Fermi liquid of constant density and within time frames on the order of 0.1 ms diffusive equilibrium is assured.

In order for the FE gas to be in diffusive equilibrium with itself, the FE diffusion length $L_X = \sqrt{D_X \tau_X}$ must be large compared to the spatial extent of the FE distribution. If we approximate the bottom of the strain induced potential well with a parabola $U = \alpha r^2$ then at temperature T the spatial extent of the gas of FE's is characterized by $\alpha(\Delta r)^2 = kT$ or $\Delta r = \sqrt{kT/\alpha}$. Taking worst case values of α and τ_X from our data, we find $L_X/\Delta r \gtrsim 450$. So the FE gas is in diffusive equilibrium with itself to a very good approximation.

In the limit of infinite FE and EHL lifetimes, the FE density at the EHL surface is

$$n_X(R_L) = \frac{1}{V_Q} e^{-\phi/kT}$$

where $V_Q = \left(\frac{2\pi\hbar^2}{m_X kT}\right)^{3/2}$, m_X = FE translational mass, ϕ = difference in binding energy per e-h pair between FE and EHL, and R_L = EHL droplet radius.

The equilibrium flux of e-h pairs into and out of the EHL droplet surface in this limit are equal and given by

$$J_\infty = \frac{4\pi m_X}{h^3} S(kT)^2 e^{-\phi/kT} \qquad (13)$$

where S = fraction of FE incident on EHL droplet that are absorbed.

In the case of finite FE and EHL lifetimes, the fluxes of e-h pairs J_{in} and J_{out} into and out of the EHL droplet surface are no longer equal. For decays there is a net current of e-h pairs out of the droplet which maintains the FE gas. The current outward is

$$4\pi R_L^2 \, (J_{out} - J_{in}) = \frac{N_X}{\tau_X} \tag{14}$$

In the case of steady state excitation there is a net current of e-h pairs into the droplet to counter the loss through bulk EHL decay. The current inward is

$$4\pi R_L^2 \, (J_{in} - J_{out}) = \frac{\frac{4}{3}\pi R_L^3 n_L}{\tau_L} \tag{15}$$

To be able to treat these systems as in quasi-equilibrium, we must have

$$\left| \frac{J_{out} - J_{in}}{J_\infty} \right| << 1, \tag{16}$$

otherwise transport must be taken into account.

We generally make measurements on an EHL droplet with a radius in the range of 20 μm to 150 μm. From Eqns. (13) and (14) using worst case values for decays

$$\left| \frac{J_{out} - J_{in}}{J_\infty} \right| \lesssim 4.9 \times 10^{-3} \text{ independent of } \phi.$$

From Eqns. (13) and (15) using worst case steady state values

$$\left| \frac{J_{out} - J_{in}}{J_\infty} \right| \lesssim \begin{cases} 4.5 \times 10^{-4} \text{ for } \phi = 1 \text{ meV} \\ 3.1 \times 10^{-5} \text{ for } \phi = 0.5 \text{ meV} \end{cases}$$

So the FE, EHL droplet system used in this experimental geometry is accurately described as being in thermal and diffusive equilibrium in both steady state and decay experiments.

IV. EXPERIMENTAL DETAILS

An ultrapure, $N_A - N_D \approx 2 \times 10^{11}$ cm^{-3}, dislocation free Ge crystal with dimensions 3 x 4 x 4 mm^3 was used. A strain induced potential well was created inside the crystal by applying an inhomogeneous stress along a ⟨111⟩ crystal direction with a spherical Delrin plunger. An infrared vidicon, television monitor set-up was used to show the well bottom to be at least 1 mm away from any crystal surface. This experimental geometry has the advantage of providing well defined FE and EHL spatial distributions isolated from crystal surfaces with at most one EHL droplet in the well.

All measurements were performed with the crystal immersed in liquid helium below the λ-point ($2.15K < T < 2.17K$). This avoids scattering of luminescence by helium bubbles. At these temperatures the EHL is less compressible and the FE gas is restricted to a smaller volume in the well bottom than is the case for higher temperatures; and the temperature is not so low that we can't measure FE luminescence below EHL threshold for modest to high stresses.

Data was taken for a range of stresses from 6 to 15 kg/mm^2 corresponding to EHL wavelength peak positions from 1.754 μm to 1.771 μm. The bottom of the strain induced potential well can be approximated by a parabola $U(r) \approx \alpha r^2$. A typical value of α is 2 meV/mm^{-2}.

A schematic of the experimental apparatus is shown in Figure 1. Steady state volume excitation of the crystal was achieved with a feedback stabilized tungsten lamp followed by a silicon filter and 1.59 μm interference filter. The luminescence was mechanically chopped, spectrally resolved, and detected by a liquid nitrogen cooled germanium PIN photodiode.

The detector output is amplified, lockin detected, and digitally integrated in the microcomputer which controls the experiment. The microcomputer automates measurements where wavelength, spatial position, or excitation power are varied.

For transient measurements a liquid nitrogen cooled GaAs laser is used for pulsed excitation and a waveform digitizer captures the full range of each decay. The microcomputer integrates the results of many pulses of the experiment. The waveform digitizer is what makes this experiment possible. If a boxcar integrater is used instead and you want to sample the decay curve at 100 points, then the boxcar is 100 times slower. With each pulse of the laser the boxcar looks at only 1% of the curve, while the waveform digitizer can look at 100%. Measurements which now take 1/2 hour with the waveform recorder would take 50 hours with a boxcar.

V. DATA

A typical set of decay data is shown in Figure 2. Plotted semilog vs time are the EHL (a), FE (b), and FE plus EHL (c) luminescence intensities. The measured decay curves for the FE-EHL system contain an EHL threshold time past which the EHL droplet no longer exists. The EHL threshold time is evident from the disappearance of the EHL decay curve (a) into the noise and the kink in the FE curve (b) due to the sudden loss of a FE source (the EHL droplet). The spectrometer grating used to spectrally resolve the EHL (a) and FE (b) luminescence was replaced with a mirror to measure the total (FE plus EHL) luminescence decay curve (c). The EHL curve (a) shows a transition from dominance of bulk EHL decay to a dominance of surface losses through FE evaporation as the surface to volume ratio of the EHL droplet increases with time. A faster than

exponential FE decay is seen past the EHL threshold time in curves (b) and (c).

A FE lifetime just below threshold and a bulk EHL lifetime are determined from the decay data for each stress. The decay curves of Figure 2 correspond to a stress of $\alpha \simeq 9$ kg/mm^2.

A typical set of luminescence intensity vs excitation power data, used to determine $\frac{\varepsilon_{RL}\ \varepsilon_{CL}}{\varepsilon_{RX}\ \varepsilon_{CX}}$, is shown in Figure 3. The EHL (a) and FE (b) curves help accurately locate EHL droplet threshold while the slopes of the FE plus EHL curve (c) above and below threshold yield the product of the EHL to FE radiative and collection efficiency ratios. The collection efficiency ratio due to the luminescence detection system's wavelength and polarization response is independently measured enabling the radiative efficiency ratio $\frac{\varepsilon_{RL}}{\varepsilon_{RX}}$ to be isolated.

No EHL formation hysteresis is observed. The EHL threshold, whether approached by lowering excitation power or increasing excitation power, is reached at the same power within our experimental resolution.

Since the FE decay curves are nonexponential, the measured decay rate $\frac{1}{\tau_X}$ depends on where along the curve it is measured. Similarly the FE radiative efficiency $\varepsilon_{RX} = \frac{\tau_X}{\tau_{RX}}$ part of $\frac{\varepsilon_{RL}}{\varepsilon_{RX}}$ depends on where below EHL threshold the slope of the power scan is measured. In order for the product $\left(\frac{1}{\tau_X}\right)(\varepsilon_{RX})$ to yield $\frac{1}{\tau_{RX}}$, care must be taken that both measurements be made the same distance below threshold.

VI. RESULTS

The results, tabulated in graph form, are displayed in Figure 4 in a plot of the enhancement factor $g_{eh}(o)$ vs $r_S = \frac{1}{a_X}\ \frac{3}{4\pi n_L}^{1/3}$. The solid and dashed lines are the results of several many body approximations for the

enhancement factor with an electron, hole mass ratio of one for a model system in which isotropic electron and hole bands are assumed. The solid curve (a) is the average result of two closely spaced approximations, one of which takes into account multiple scatterings to infinite order between all components of the plasma. The dashed curve (b) is the average result of the Hubbard and random phase approximations which are closely spaced over the range of r_S shown. Our preliminary results, plotted as solid dots, show no striking agreement with either curve. That none of the calculations for these curves included the electron-hole band anistropy may have some bearing on this disagreement. Vashishta et al.[1] claim that for the EHL binding energy per e-h pair ϕ anisotropy is as large an effect as multiple scattering. If this carries over for the enhancement factor, then calculations taking into account electron hole band anisotropy are necessary.

Vashishta et al.[1] have for the infinite ⟨111⟩ stress limit made a calculation of $g_{eh}(o)$ including anisotropy and find $g_{eh}(o) = 6.8$ corresponding to a density of 1.11×10^{16} cm^{-3} or $r_S = 1.57$. Our data extrapolated to $r_S = 1.57$ are not inconsistent with this finding.

REFERENCES

[1]P. Vashishta, P. Bhattacharyya, K. S. Singwi, Phys. Rev. B 10, 5108 (1974).

[2]H.-h. Chou and George K. Wong, Phys. Rev. Lett. 41, 1677 (1978).

[3]S. M. Kelso and J. E. Furneaux, Solid-State Electron. 21, 1377 (1978).

[4]C. Benoit a la Guillaume and M. Voos, Phys. Rev. B 7, 1723 (1973).

[5]R. S. Markiewicz, J. P. Wolfe and C. D. Jeffries, Phys. Rev. B 15, 1988 (1977).

[6]J. P. Wolfe, R. S. Markiewicz, S. M. Kelso, J. E. Furneaux, and C. D. Jeffries, Phys. Rev. B 18, 1479 (1978).

FIGURE CAPTIONS

FIGURE 1. Microcomputer controlled experimental apparatus. A light source at the left photo-excites a Ge crystal at liquid He temperatures. The luminescence is collected by the output lens and focussed on the slit plane of the spectrometer. Radiation of the wavelength selected by the spectrometer is detected by an N_2-cooled Ge photodiode. The electronic signal is then routed to a transient recorder for pulsed experiments or a lockin for steady state experiments. For pulsed experiments an N_2-cooled GaAs laser is used. For steady state experiments either an argon laser or a suitably filtered incandescent lamp is used. The microcomputer controls the feedback stabilized steady state light sources. It also controls the output lens position and the spectrometer wavelength drive, thus automating spatial and wavelength resolved luminescence measurements.

FIGURE 2. Luminescence decay curves. Luminescence intensity is plotted semilog vs time in ms for the electron-hole liquid droplet (a), free exciton gas (b), and the total luminescence (c) with no spectral resolution. The electron-hole liquid droplet has disappeared by 4 ms.

FIGURE 3. Luminescence intensity vs excitation power. Luminescence intensity is plotted vs excitation power for the electron-hole liquid droplet (a), free exciton gas (b), and the total luminescence (c). The electron-hole liquid threshold is clearly visible in curves (a) and (b). All curves are scaled vertically to have the same height.

FIGURE 4. The enhancement factor $g_{eh}(o)$ is plotted vs. r_S where $r_S = \frac{1}{a_X}\left(\frac{3}{4\pi n_L}\right)^{1/3}$, a_X being the free exciton Bohr radius and n_L the electron-hole liquid density. The dots are our data while the curves are theoretical results for a model system taken from Ref. 1 which does not include electron-hole band anisotropies. Unstressed Ge corresponds to $r_S = .57$. Reference 1 predicts for the infinite ⟨111⟩ stress limit $g_{eh}(o) = 6.8$ and $r_S = 1.57$ with electron, hole band anisotropies included.

Fig. 1

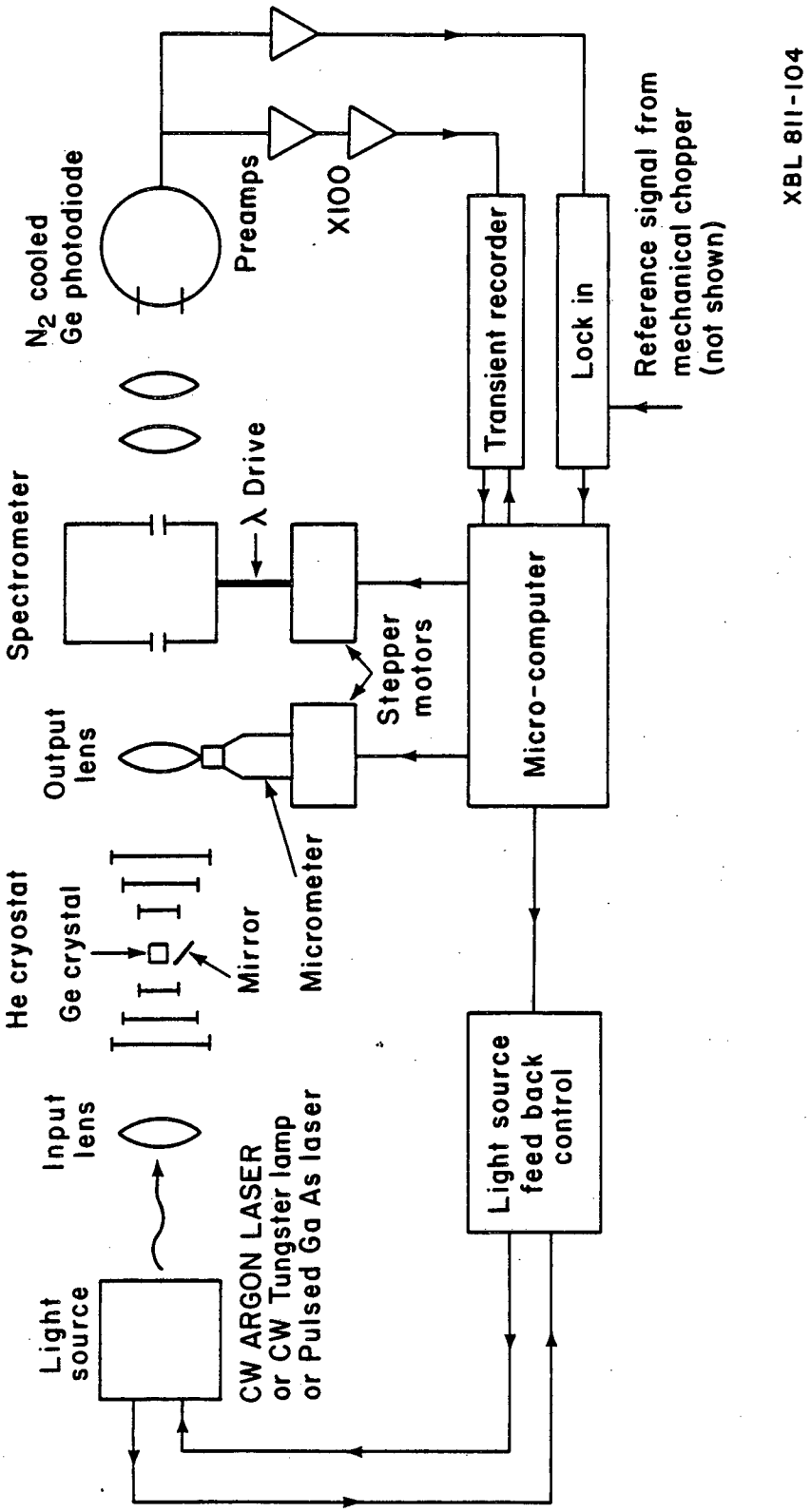
Light source
CW ARGON LASER
or CW Tungster lamp
or Pulsed Ga As laser
Input lens
He cryostat
Ge crystal
Mirror
Micrometer
Output lens
Spectrometer
λ Drive
Stepper motors
Micro-computer
Light source feed back control
Transient recorder
Lock in
Reference signal from mechanical chopper (not shown)
Preamps
X100
N_2 cooled Ge photodiode
XBL 811-104

Fig. 2

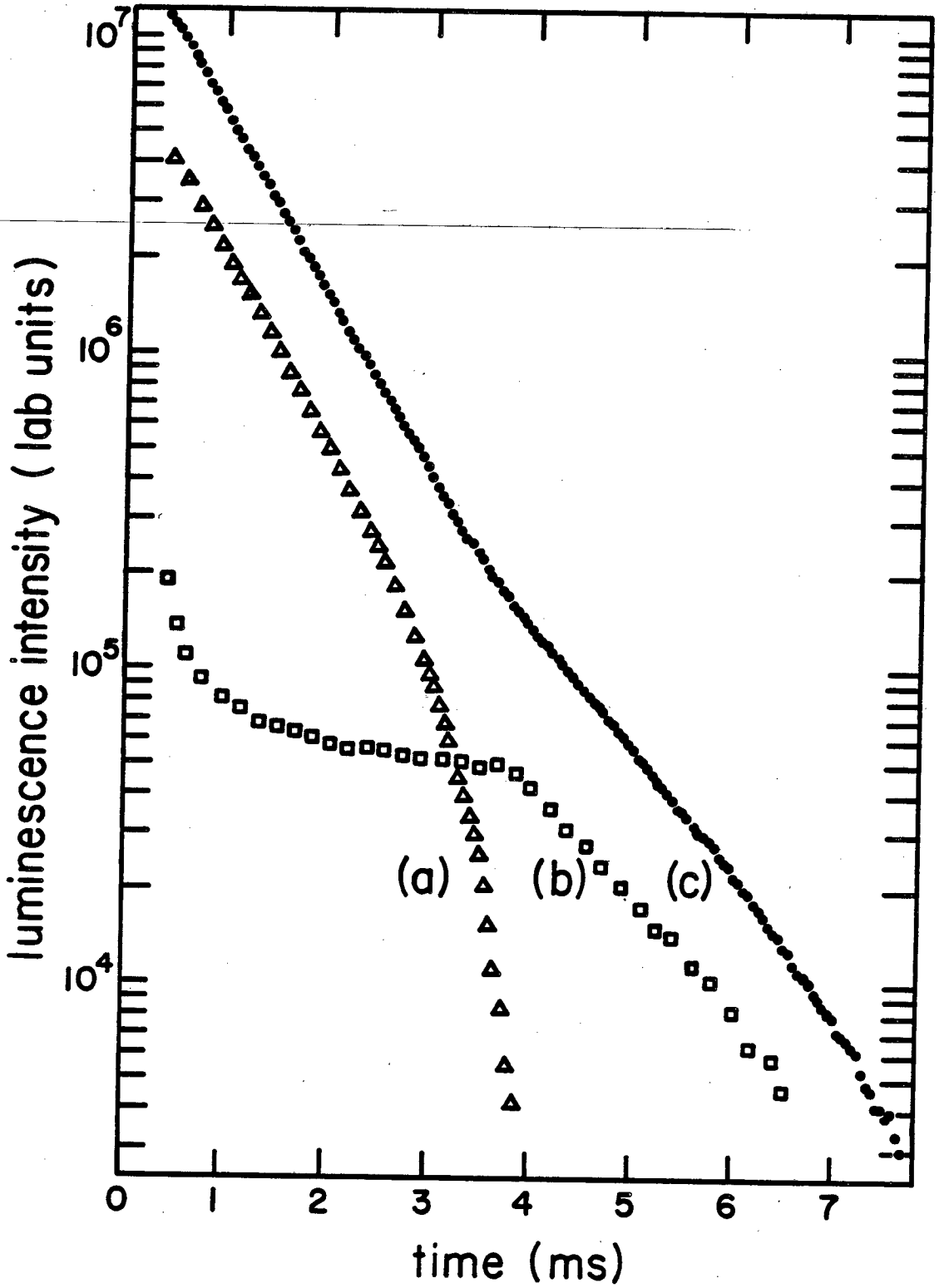

XBL 8112-12787

Fig. 3

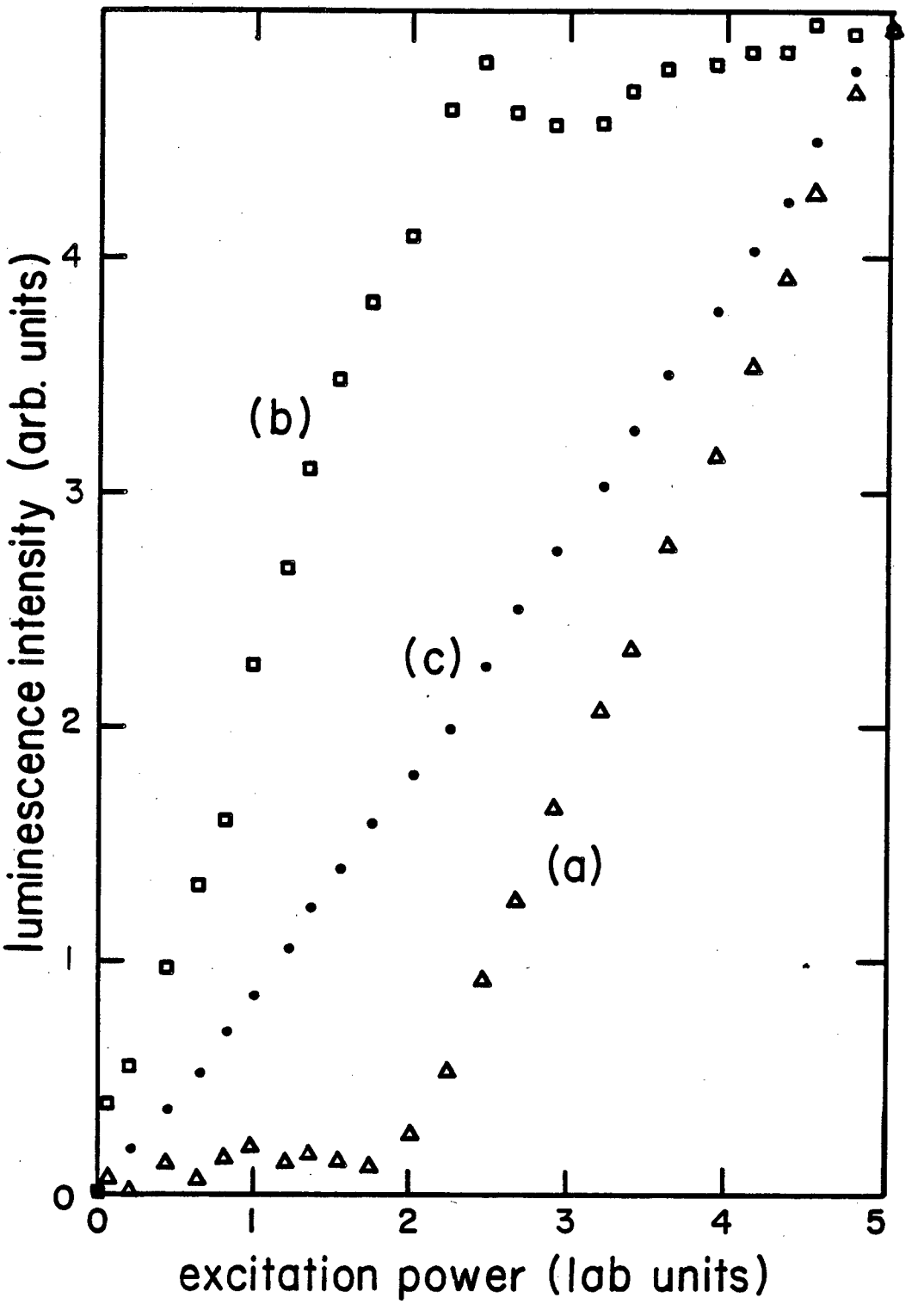

XBL 8112-12786

Fig. 4

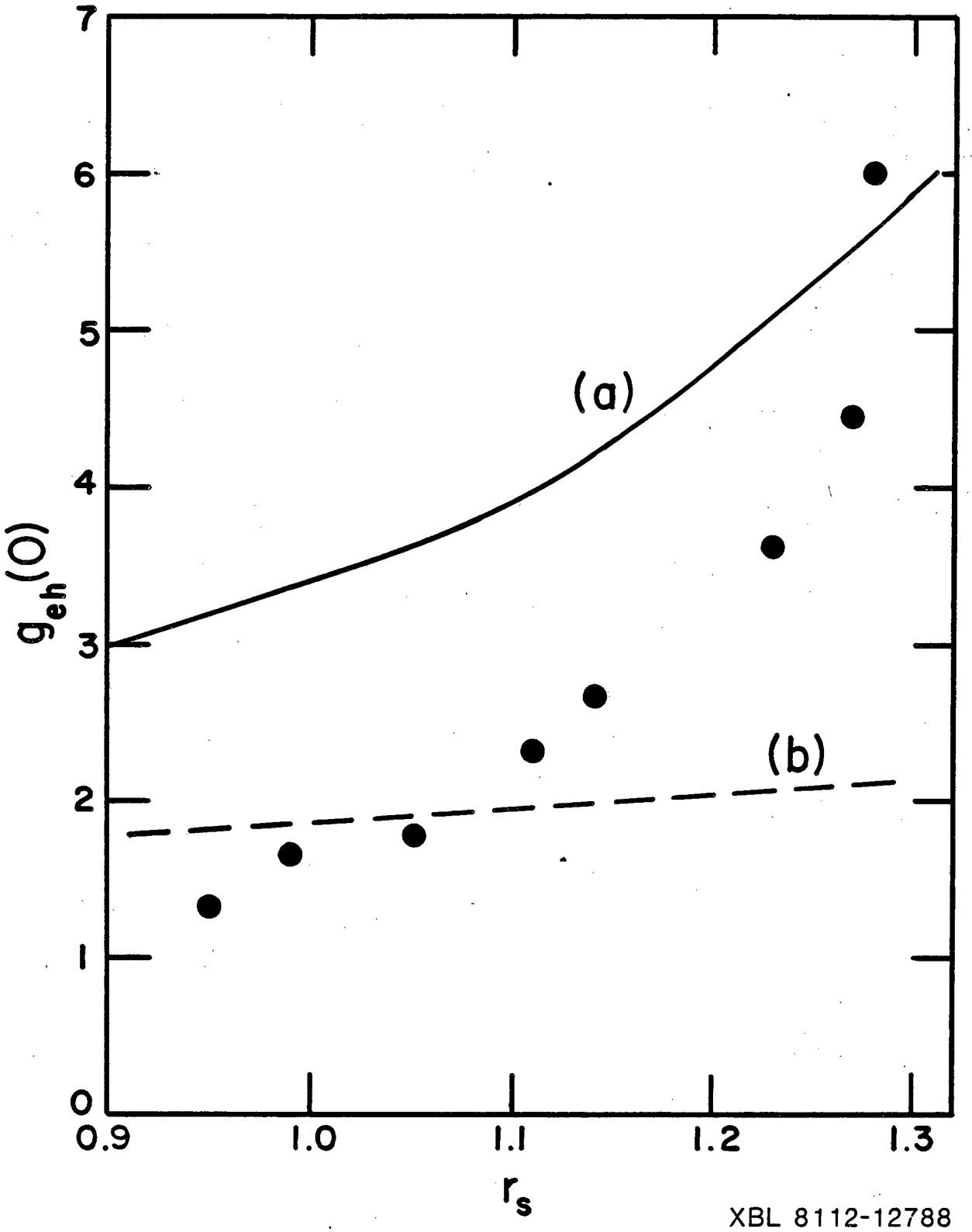

This report was done with support from the Department of Energy. Any conclusions or opinions expressed in this report represent solely those of the author(s) and not necessarily those of The Regents of the University of California, the Lawrence Berkeley Laboratory or the Department of Energy.

Reference to a company or product name does not imply approval or recommendation of the product by the University of California or the U.S. Department of Energy to the exclusion of others that may be suitable.

TECHNICAL INFORMATION DEPARTMENT
LAWRENCE BERKELEY LABORATORY
UNIVERSITY OF CALIFORNIA
BERKELEY, CALIFORNIA 94720